2021 IEEE Energy Conversion Congress and Exposition (ECCE) | 978-1-7281-5135-9/21/$31.00 ©2021 IEEE | DOI: 10.1109/ECCE47101.2021.9595140

Implementation of an Isolated Phase-Modular-Designed Three-Phase PFC Rectifier Based on Single-Stage LLC Converter

Mojtaba Forouzesh, *Student Member*, *IEEE*, Yan-Fei Liu, *Fellow, IEEE*, Paresh C. Sen, *Life Fellow, IEEE*

Department of Electrical and Computer Engineering, Queen's University, Kingston, ON, Canada
Email: m.forouzesh@queensu.ca, yanfei.liu@queensu.ca, senp@queensu.ca

***Abstract*— This paper proposes a new phase-modular three-phase single-stage rectifier based on the LLC resonant converter. The proposed rectifier provides power factor correction, output voltage regulation, and electrical isolation in a single-stage modular-designed approach. The proposed rectifier has minimal switching loss due to the ZVS and ZCS operations of all the switches and diodes. Moreover, the proposed AC-DC converter does not use any bulky passive components and hence is suitable for high power density applications that also require high power conversion efficiency. Design notes and specifications of a single module are provided in this paper. Computer simulation results verified the unity PFC performance and output voltage regulation using a small output capacitance without any low-frequency ripple. Furthermore, the feasibility of the proposed rectifier is validated by the experimental results of a digitally implemented GaN-based laboratory prototype.**

Keywords—Three-phase rectifier, modular-designed, phase-modular, isolated AC-DC converter, power factor correction (PFC), unity power factor, single-stage LLC AC-DC converter, GaN HEMTs.

I. INTRODUCTION

When high power conversion from the AC mains to a DC load is required, three-phase rectifiers are preferred solutions. For example, high-power three-phase rectifiers are required in a 400 Vdc power distribution system for telecommunications and datacenters applications [1]. Moreover, to charge the high voltage battery in electric vehicles (EVs) with a DC fast charging approach, a high-power rectifier connected to the three-phase main is required [2]. Three-phase rectifiers are either boost-type or buck-type, and in some cases, with universal input systems, a buck-boost type may be employed [3].

In both above-mentioned applications, some main features are required such as high power factor correction (PFC), regulated output voltage, high conversion efficiency, and electrical isolation if needed by the system due to safety purposes. The output voltage of three-phase boost-type rectifiers like Vienna Rectifier (i.e. 700 V – 800 V) is usually higher than the load level DC bus and hence usually an additional step-down conversion is required [3]. On contrary, three-phase buck-type rectifiers can provide a wide output voltage regulation without compromising the PFC. However, input filter capacitors consume reactive power, and the semiconductors should withstand line to line voltages in two-level buck-type rectifiers like in a Swiss Rectifier [4]. Nevertheless, these boost-/buck-type rectifiers lack the voltage isolation that is required for direct connection to some loads.

Three-level boost rectifiers such as Vienna Rectifiers are one of the most popular three-phase rectifiers to be used for PFC purposes in two-stage converters, which is due to their reduced voltage stresses and hence smaller boost inductor, EMI requirements, and low switching losses [3]. At the second stage, a soft-switching DC-DC converter like the LLC converter or phase-shifted full-bridge converter can be used to efficiently provide the output voltage regulation and isolation [5] and [6]. The main problem related to the mentioned two-stage approach is the existence of two separate conversion stages with a relatively large dc-link capacitor in between that carries a low-frequency current ripple. Those limitations lead to a low power density and low overall conversion efficiency for the AC-DC converter.

Recently, single-stage rectifiers have gained a lot of attention as they can potentially achieve higher power density and efficiency than two-stage approaches. In [7], a new three-phase rectifier is proposed based on a dual active bridge (DAB) converter with three-winding coupled inductors and individual input inductors for each phase. In [8], a soft-switched DAB-based single-stage three-phase converter is proposed for EV application. Two back-to-back switches are used for each phase leg to withstand the line voltage and a single bulky transformer is used for the three-phase rectifier to connect to the secondary side. In [9], another three-phase single-stage rectifier is proposed with only nine switches at the input and three transformers to connect to the DC side. All the mentioned three-phase converters require complex control implementation using direct-quadrature-zero (DQZ or DQ0) transformation, and some of them require a large number of passive components such as multi-winding coupled inductors and DC-link capacitors, and large EMI suppression components.

Another interesting solution for three-phase rectifiers is a phase-modular approach. In [10]-[12], some three-phase single-stage isolated rectifiers are proposed based on SEPIC and Cuk converters that mostly use an input inductor with DCM operation to achieve PFC. Although control of these kinds of rectifiers is like a DC-DC converter, it is not suitable for high-power applications due to the large loss in the passive components. In [13], the design of a phase-modular three-phase rectifier is provided for welding power supply. The proposed converter uses a push-pull structure with active power factor correction to achieve sinusoidal input current. Since a proper design of the push-pull transformer is not easy to achieve and usually not so efficient, the proposed rectifier is not suitable for high power applications. In [14], a three-phase high power density rectifier is proposed based on a single-stage DAB converter. A new triple phase shift control is introduced to be able to perform PFC properly around the zero voltage crossing points. Hence, the control variables are switching frequency and three different phase shifts between the switching legs, which make the control approach complex. Moreover, the introduction of additional phase shifts in the DAB converter often increases the root mean square (RMS) current and hence conduction loss as well as the switch dead-band and turn-off losses.

Despite resonant converters have been widely used in DC-DC applications over the past decades [15]-[20], there is not enough research around their operation in AC-DC applications. Recently, a few papers have discussed the active PFC functionality of the LLC resonant converter with a single-stage approach for single-phase AC-DC applications [21]-[23].

In this paper, a new three-phase single-stage rectifier is proposed in a phase-modular approach using the LLC resonant converter to take advantage of ZVS and ZCS operations for the switches. In the proposed rectifier the power conversion loss is mainly conduction losses through components which make the proposed rectifier suitable for high power applications. Moreover, there is no need for bulking output capacitor as the output capacitor does not carry any low line-frequency ripple. The main operation of the proposed rectifier is discussed in the next section, and the design criteria for a single module at different operating conditions are discussed in Section III. Computer simulation and experimental results are provided in Section IV to verify the operation of the proposed rectifier. Finally, this paper is concluded in Section V.

II. The Proposed Three-Phase Rectifier

Fig. 1 illustrates the proposed phase-modular three-phase single-stage LLC AC-DC converter. Each module comprises a single-stage LLC converter operating in PFC mode. The hole three-phase rectifier consists of three LLC modules that are controlled independently to provide PFC in the three-phase system. In the proposed topology one-third of the total output power is processed in parallel in each phase and hence the efficiency of the whole system is equal to the conversion efficiency of each module. Since LLC resonant converter is used in each module, the switching loss through the switches and diodes is negligible and most of the power loss is conduction losses. Moreover, no input inductor or DC link capacitor is used in the proposed topology. It can be observed from Fig. 1 that the output voltage of each phase has a double line frequency ripple due to the pulsating input power on each phase. In a three-phase system with a 120° degree phase shift between phases, the output voltage ripple of each phase is 120° degrees apart from each other and hence the low-frequency components get canceled out in the output and the total output voltage does not have any line frequency voltage ripple.

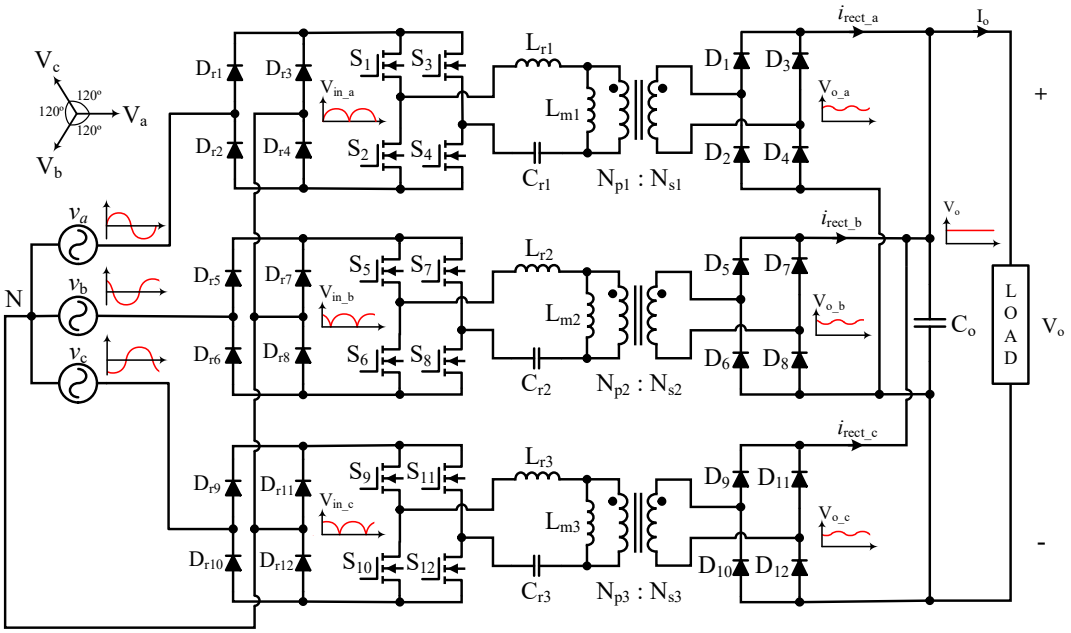

Fig. 1. The proposed phase-modular three-phase single-stage rectifier.

The grid voltages (v_a, v_b, v_c) of the three-phase system are defined as follows:

$$\begin{cases} v_a(t) = \sqrt{2}V_a \sin(\omega t) \\ v_b(t) = \sqrt{2}V_b \sin(\omega t - 120°) \\ v_c(t) = \sqrt{2}V_c \sin(\omega t + 120°) \end{cases} \quad (1)$$

where V_a, V_b, V_c are the root mean square (RMS) value of the AC input voltage (V_{ac}), which are equal in a balanced three-phase system. ω is the angular line frequency that is defined as follows:

$$\omega = 2\pi f_{line} \quad (2)$$

where f_{line} is the grid AC frequency. Considering a unity power factor, the grid currents (i_a, i_b, i_c) can be represented as follows:

$$\begin{cases} i_a(t) = \sqrt{2}I_a \sin(\omega t) \\ i_b(t) = \sqrt{2}I_b \sin(\omega t - 120°) \\ i_c(t) = \sqrt{2}I_c \sin(\omega t + 120°) \end{cases} \quad (3)$$

where I_a, I_b, I_c are the RMS value of the AC input current (I_{ac}), which are equal in a balanced three-phase system.

The rectified input voltage in each phase has the following form:

$$\begin{cases} v_{in-a}(t) = \sqrt{2}V_a|\sin(\omega t)| \\ v_{in-b}(t) = \sqrt{2}V_b|\sin(\omega t - 120°)| \\ v_{in-c}(t) = \sqrt{2}V_c|\sin(\omega t + 120°)| \end{cases} \quad (4)$$

The rectified output current in each phase has an average value (i_{avg-ph}) plus a high-frequency term (i_{HF-ph}) as follows:

$$\begin{cases} i_{rect-a}(t) = i_{avg-a}(t) + i_{HF-a}(t) \\ i_{rect-b}(t) = i_{avg-b}(t) + i_{HF-b}(t) \\ i_{rect-c}(t) = i_{avg-c}(t) + i_{HF-c}(t) \end{cases} \quad (5)$$

Assuming the switching frequency is very large, and the energy stored in the output capacitor is negligible, then the instantaneous input power equals the instantaneous output power. Hence, the high-frequency term of the rectified current is neglected, and the average output current of each phase can be written as follows:

$$\begin{cases} i_{avg-a}(t) = \dfrac{v_a(t) \times i_a(t)}{V_o} \\ i_{avg-b}(t) = \dfrac{v_b(t) \times i_b(t)}{V_o} \\ i_{avg-c}(t) = \dfrac{v_c(t) \times i_c(t)}{V_o} \end{cases} \quad (6)$$

where V_o is the output voltage that is pure DC for a balanced three-phase system. Hence, the output current is the sum of the three rectified currents as follows:

$$I_o = i_{avg-a}(t) + i_{avg-b}(t) + i_{avg-c}(t) \quad (7)$$

$$\begin{aligned} \rightarrow I_o &= \frac{V_{ac}I_{ac}}{V_o}(1 - \cos(2\omega t)) \\ &+ \frac{V_{ac}I_{ac}}{V_o}(1 - \cos(2\omega t - 240°)) \\ &+ \frac{V_{ac}I_{ac}}{V_o}(1 - \cos(2\omega t + 240°)) \\ &= 3\frac{V_{ac}I_{ac}}{V_o} \end{aligned}$$

III. Design Considerations for a Single Module

A. Power Factor Correction (PFC) Gain Requirement

The per-unit AC grid voltage and current of a unity power factor correction (PFC) converter over half line cycle is shown in Fig. 2. The AC voltage and current have the following forms:

$$\begin{aligned} v_{ac}(\theta) &= \sqrt{2}V_{ac}\sin(\theta) \\ i_{ac}(\theta) &= \sqrt{2}I_{ac}\sin(\theta) \end{aligned} \quad (8)$$

where θ is the line cycle angle that defines the AC value over a full line cycle from 0° to 360°.

Moreover, the instantaneous AC power has the following form that is illustrated in the middle row of Fig. 2.

$$p_{ac}(\theta) = v_{ac}(\theta) \times i_{ac}(\theta) = P_o \times 2\sin(\theta)^2 \quad (9)$$

It can be observed that the AC power is pulsating in a PFC rectifier and the peak value is happening at θ=90°, which for a lossless circuit is equal to two times of the average output power ($2P_o$). For a DC output voltage, the required line cycle voltage gain of a PFC converter ($G_{req}(\theta)$) can be found as:

$$G_{req}(\theta) = \frac{V_o}{v_{ac}(\theta)} = \frac{V_o}{\sqrt{2}V_{ac}\sin(\theta)} \quad (10)$$

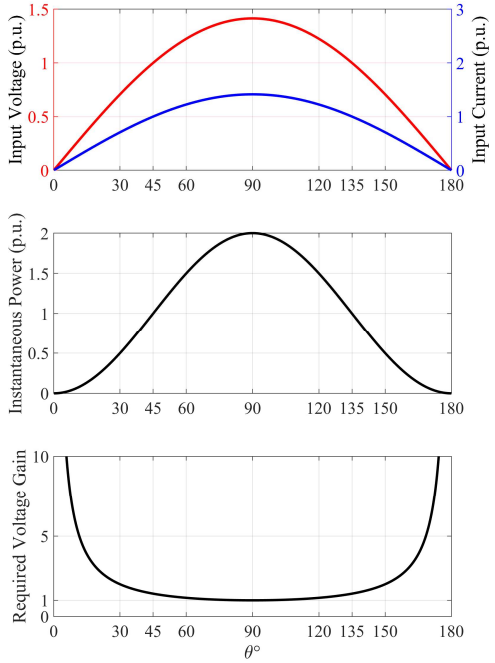

Fig. 2. Basic pulsating characteristics of PFC converters over a half line cycle.

Considering the output voltage is equal to the peak grid voltage, the required voltage gain can be drawn as in the third row of Fig. 2. The minimum required voltage gain occurs at θ=90º and the required voltage gain close to grid voltage zero-crossing points (i.e. θ=0º and 180º) is very large. Hence, a candidate converter should be able to provide a relatively large voltage gain variation over the quarter line cycle back and forth. In the single-stage LLC converter with PFC functionality, the impedance of the resonant tank should change in a way to satisfy the gain requirement due to input voltage variation over the half-line cycle.

B. LLC Resonant Tank Design for PFC Application

The voltage gain of LLC resonant converter that is frequency dependant can be found as follows:

$$G_{LLC}(f_{sw}) = \frac{1}{\sqrt{\left[1+\frac{1}{K}\left(1-\frac{1}{{f_n}^2}\right)\right]^2 + \left[\left(f_n-\frac{1}{f_n}\right)Q\right]^2}} \quad (11)$$

where K is the inductance ratio and is defined as $K = L_m/L_r$, and f_n is the frequency ratio and is defined as $f_n = f_{sw}/f_s$. Moreover, the series resonant frequency (f_s), parallel resonant frequency (f_p), quality factor (Q), and the equivalent load resistance transferred to the primary side of the transformer (R_{oe}) in LLC converter can be calculated from the following equations:

$$f_s = \frac{1}{2\pi\sqrt{L_r C_r}} \quad (12)$$

$$f_p = \frac{1}{2\pi\sqrt{(L_r+L_m)C_s}} \quad (13)$$

$$Q = \sqrt{\frac{L_r}{C_r}} \times \frac{1}{R_{oe}} \quad (14)$$

$$R_{oe} = \frac{8n^2}{\pi^2} \times R_L \quad (15)$$

Fig. 3 shows the voltage gain curves of the LLC converter with different quality factors. The quality factor in the LLC tank is directly related to the output load and when the quality factor decreases in Fig. 3, the voltage gain of the LLC tank increases, which is in accordance with the required characteristics of a PFC circuit that is shown in Fig. 2. Close to line voltage zero-crossing points (i.e. θ=0°,180°), the input voltage and current are small and so the output power is equivalent to a large load resistance, hence the voltage gain of the LLC converter should be high for this case. Close to maximum line voltage (i.e. θ=90°) the input voltage and current are large and so the output power is maximum which is equivalent to a small load resistance, hence the voltage gain of the LLC converter should be low for this case. To remain below the series resonant frequency to benefit from ZCS for the output diodes, the minimum voltage gain of the LLC tank could be set at unity for the maximum input line voltage.

As it is demonstrated in Fig. 3 if the switching frequency of the LLC converter changes back and forth between the parallel and series resonant frequencies (f_p<f_{sw}<f_s), the voltage gain requirements at both zero crossing line voltages and maximum line voltages can be fulfilled. The colored region in Figure 3 would be the desirable PFC operating range of the LLC converter and the dashed black line is the margin of the voltage gain of the LLC tank in PFC mode. Depending on the required output voltage level, the operating frequency of the LLC converter can be between f_p and a higher frequency but below the f_s that will be within the operating colored region that is shown in Fig. 3.

The total theoretical input to the output voltage gain of the full-bridge LLC converter can be calculated as follows:

$$G_{LLC-total}(f_{sw}) = \frac{1}{n} \times G_{LLC}(f_{sw}) \quad (16)$$

where n is the turn ratio of the transformer and is defined as $n = N_{pri}/N_{sec}$.

The first step of the design procedure for an LLC converter in a PFC application is to find the transformer turn ratio (n) based on the input voltage and output voltage. From the bottom row in Fig. 2, it can be inferred the minimum required voltage gain in PFC application is occurred at $\theta = 90^{\circ}$ where the input voltage is at its peak value. Therefore, the transformer turn ratio (n) can be found in a way that the minimum voltage gain requirement is achieved at the series resonant frequency (f_s) operation of LLC tank with a unity voltage gain, which is the maximum operating frequency that is desirable in the inductive region.

$${G_{req}}^{min}(\theta) = G_{req}(90°) = \frac{V_o}{\sqrt{2}V_{ac}} \quad (17)$$

$${G_{LLC(total)}}^{min}(f_{sw}) = G_{LLC(total)}(f_s) \quad (18)$$

$$\rightarrow G_{req}(90°) = G_{LLC}(f_s) \times \frac{1}{n} \rightarrow n = \frac{\sqrt{2}V_{ac}}{V_o} \quad (19)$$

For PFC operation, the equivalent load resistance is no longer a constant value as the instantaneous output power is changing with respect to the line phase angle (θ). The AC equivalent circuit of the LLC converter in PFC operation is illustrated in Fig. 4.

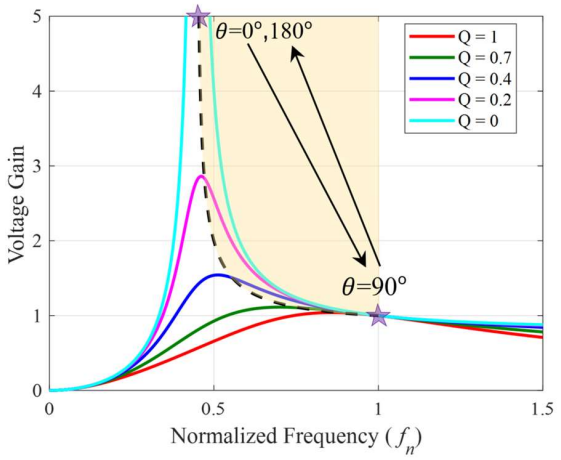

Fig. 3. Voltage gain curves of LLC converter for different quality factors.

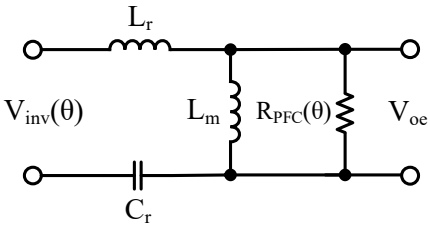

Fig. 4. The equivalent AC model of LLC converter for PFC operation.

Considering a lossless power circuit, equation (9) can be rewritten as follows:

$$p_o(\theta) = P_o \times 2\sin^2(\theta) = \frac{{V_{oe}}^2}{R_{oe\_FL}} \times 2\sin^2(\theta) \tag{20}$$

where V_{oe} is the equivalent output voltage transferred to the primary side of the transformer, and R_{oe_FL} is the equivalent load resistance at full load condition transferred to the primary side of the transformer, which can be calculated from (15) by substituting full load resistance (R_{L_FL}). The equivalent load resistance for the PFC operation that is line phase angle dependant is defined as $R_{PFC}(\theta)$ that can be calculated as follows:

$$R_{PFC}(\theta) = \frac{{V_{oe}}^2}{p_o(\theta)} = \frac{R_{oe\_FL}}{2\sin^2(\theta)} \tag{21}$$

The quality factor in the PFC operation can be calculated using (15) and (21) as follows:

$$Q_{PFC}(\theta) = \sqrt{\frac{L_s}{C_s}} \times \frac{1}{R_{PFC}(\theta)} = \sqrt{\frac{L_s}{C_s}} \times \frac{2\sin^2(\theta)}{R_{oe\_FL}} = 2\sin^2(\theta) \times Q_{FL} \tag{22}$$

where Q_{FL} is the full load quality factor and is calculated as:

$$Q_{FL} = \frac{\pi^2}{8n^2} \times \sqrt{\frac{L_s}{C_s}} \times \frac{P_{o\_FL}}{V_o^2} \tag{23}$$

Then the line phase angle dependent LLC tank voltage gain can be calculated by substituting (22) in (11).

$$G_{LLC}(f_{sw}, \theta) = \frac{1}{\sqrt{\left[1 + \frac{1}{K}\left(1 - \frac{{f_s}^2}{{f_{sw}}^2}\right)\right]^2 + 4\sin^2(\theta)\left[\left(\frac{f_s}{f_{sw}} - \frac{f_{sw}}{f_s}\right)Q_{FL}\right]^2}} \tag{24}$$

After the turn ratio (n) is found from the maximum AC input peak voltage and the minimum DC output voltage, the series resonant components can be found with respect to the desired maximum operating frequency that is desired to be equal to the series resonant frequency (f_s). The quality factor is set in such a way the required voltage gain at the maximum desired DC output voltage is achieved at peak line voltage ($\sqrt{2}V_{ac}$) that is corresponding to two times average output power ($2P_o$). The parallel inductor is designed in such a way as to achieve the minimum circulation current at peak power while maintaining the required voltage gain for maximum DC output voltage level.

IV. Simulation and Experimental Results

A set of parameters are designed for the proposed three-phase rectifier based on the desired output voltage and power levels. The AC input voltage is connected to a four-wire 220 V - 50 Hz system and the maximum power is achieved at the maximum output voltage level (i.e. 380 V). All the specifications and the design parameters are listed in Table I. The total used output capacitance is only 60 µF for the proposed rectifier that is considered small for an AC to DC converter of this power. Since the output capacitor has no low frequency ripple it can be realized with film capacitors that have higher reliability and longer lifetime than electrolytic capacitors.

A. Simulation Results

The proposed three-phase rectifier has been simulated in the PSIM environment with closed-loop control implementation to verify its performance. In the proposed converter three LLC modules are operating independently with three inner current loops, and hence three different switching frequencies should be employed on the three-phase modules at each operating instant. Moreover, a low bandwidth outer voltage loop is used to control the output voltage level without distorting the input current.

First, the operation of the designed LLC converter is verified for different line phase angles (θ) corresponding to different input voltages and loads. Fig. 5 shows the resonant current, magnetizing current, input bridge, and output bridge switch voltages and currents for three different line conditions for V_o=250 V. Operation at θ=90° corresponds to 2 times the average output power, operation at θ=60° corresponds to 1.5 times the average output power, and operation θ=30° corresponds to 0.5 times the average output power. From Fig. 5 it can be observed that ZVS is achieved at turn-ON for the input bridge switches and ZCS is achieved for both turn-ON and turn-OFF instants for all three line conditions. In Fig. 6, soft switching performance for the same conditions are verified through simulation for V_o=380 V. It can be observed that the

TABLE I. The Deisgn Parameters

Parameters/Descriptions		Values
Maximum Output Power (P_o)		1.5 kW
Input Voltage (V_a, V_b, V_c)		220 V_{RMS}
Line Frequency (f_{line})		50 Hz
Maximum Output Voltage (V_{o-max})		380 V
Minimum Input Voltage (V_{o-min})		250 V
Switching Frequency Range ($f_{sw[1,2,3]}$)		200 kHz - 450 kHz
Parallel Resonant Inductor ($L_{m[1,2,3]}$)		120 µH
Series Resonant Inductor ($L_{r[1,2,3]}$)		23 µH
Series Resonant Capacitor ($C_{r[1,2,3]}$)		4.8 nF
Transformer Turns Ratio ($N_{p[1,2,3]}$: $N_{s[1,2,3]}$)		13:10
Input LC Filter	Inductor ($L_{in[1,2,3]}$)	15 µH
	Capacitor ($C_{in[1,2,3]}$)	1 µF
Output Capacitor (C_o)		60 µF

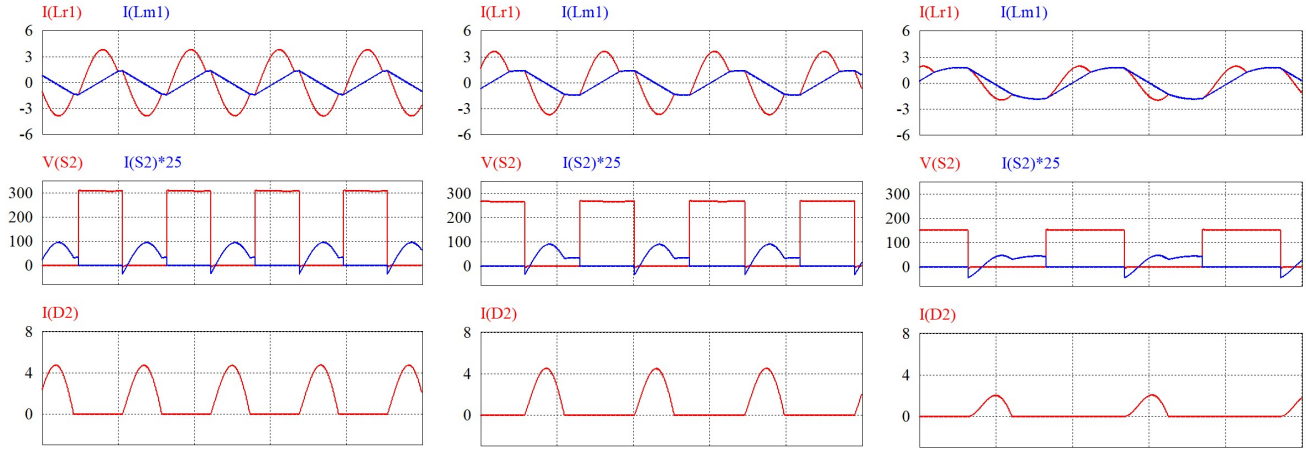

(a) θ=90° - V_{in}=311 V - f_{sw}=436 kHz (b) θ=60° - V_{in}=269 V - f_{sw}=343 kHz (c) θ=30° - V_{in}=156 V - f_{sw}=244 kHz

Fig. 5. Soft-switching performance at different input voltages (V_{in}) and line phase angles (θ) for V_o=250 V.

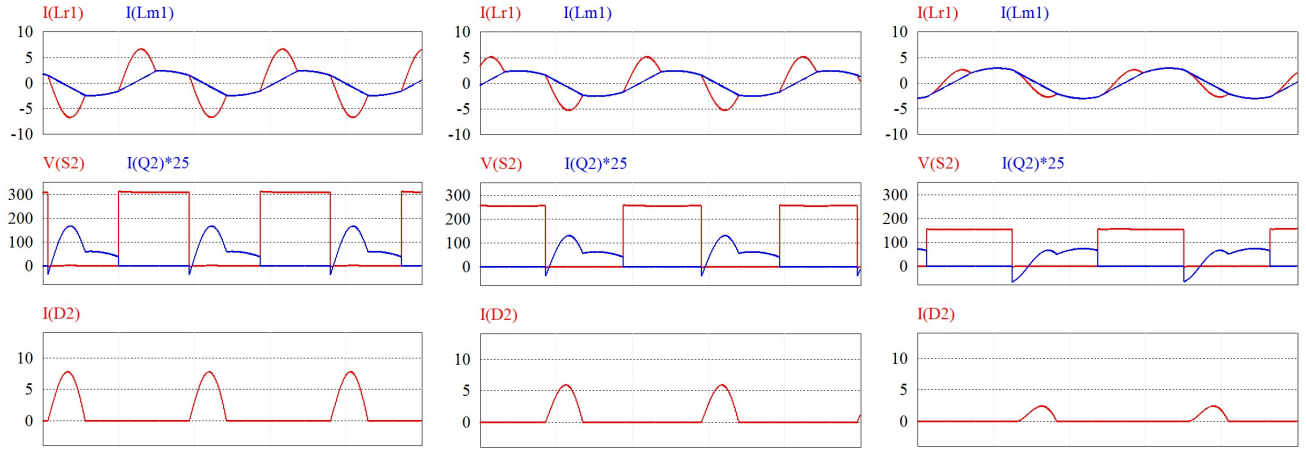

(a) θ=90° - V_{in}=311 V - f_{sw}=266 kHz (b) θ=60° - V_{in}=269 V - f_{sw}=245 kHz (c) θ=30° - V_{in}=156 V - f_{sw}=219 kHz

Fig. 6. Soft-switching performance at different input voltages (V_{in}) and line phase angles (θ) for V_o=380 V.

switching frequency varies from 436 kHz to less than 244 kHz for V_o=250 V and the switching frequency varies from 266 kHz to less than 219 kHz for V_o=380 V.

The simulation results of the three-phase operation for both output voltages are shown in Fig. 7. A unity power factor correction can be observed for both conditions. The THD is 1.9% for the case with V_o=250 V and it is 1.4% for the case with V_o=380 V. The frequency variation and its range is shown in Fig. 7 is based on the expectation and the minimum frequency (~190 kHz) is reached around zero voltage crossing for both output voltage levels. Moreover, it can be observed that the output voltage does not have any low-frequency ripple. An FFT analysis of the current through the output capacitor is shown in Fig. 8. It can be observed that there is no low-frequency component in the output capacitor current and the current ripple is only around the switching frequency. Hence, a small film capacitor can be used at the output of the proposed rectifier.

B. Experimental Results

A three-phase laboratory prototype is built for further investigation using the parameters listed in Table I. It should be mentioned that a small input LC filter is used at the input of the LLC converter in each module to filter the high-frequency switching ripple. The input current is sensed through a sensing resistor just before the input LC filter so the average input current can be sensed at each voltage line phase angle (θ). Fig. 9 shows the input voltage and current of one phase and the measured FFT of the input current in the oscilloscope to show a unity power factor correction performance. The zoomed-in experimental results at different line input voltage corresponding to different line phase angles (θ) are shown in Fig. 10. The experimentally measured results are in good agreement with the simulation results shown in Fig. 5. In the prototype, an approximate efficiency measurement shows the peak efficiency is more than 96.5 % and the peak power factor is more than 0.998. It should be mentioned that the estimated theoretical efficiency for the same condition was around 97.4 %, which can be further improved by around 1 % after changing the input and output diodes with MOSFETs.

V. CONCLUSION

In this paper, a new three-phase rectifier with single-stage power processing was introduced. An LLC converter module was used on each phase so ZVS and ZCS is achieved for all

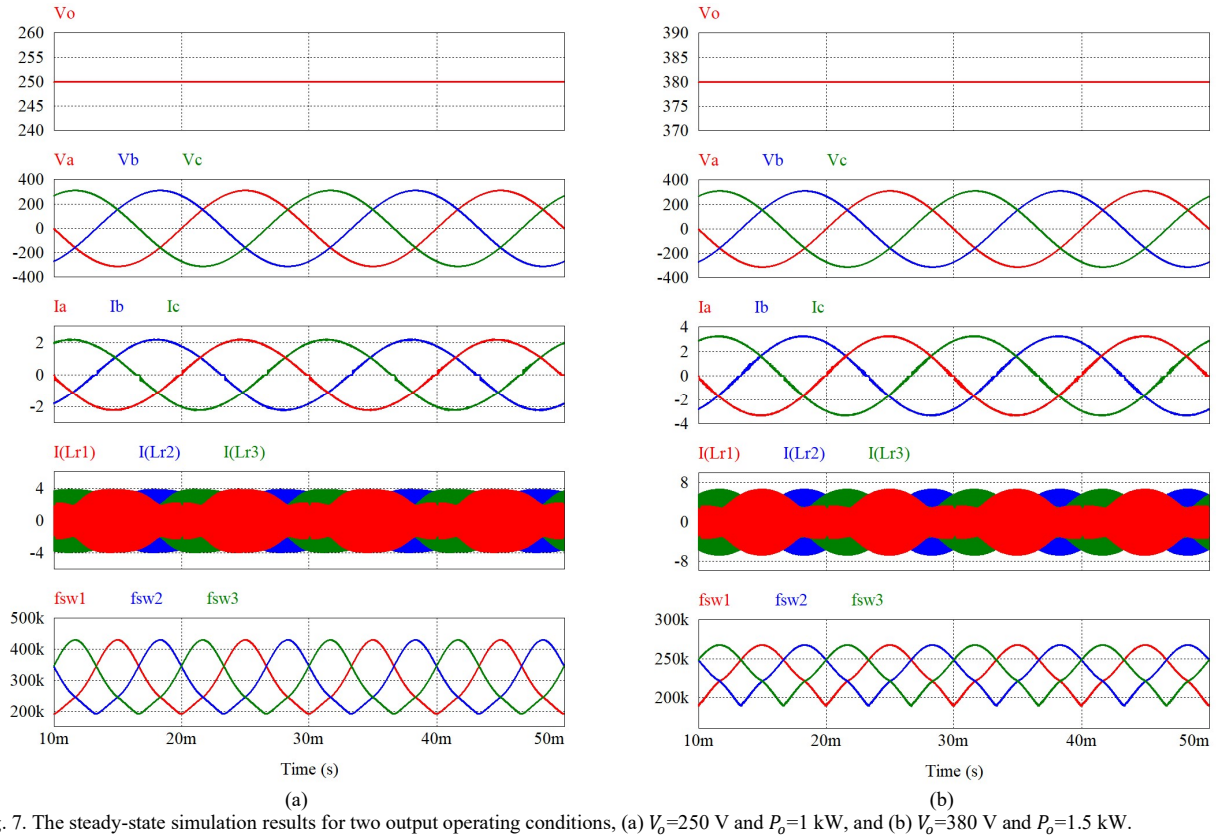

Fig. 7. The steady-state simulation results for two output operating conditions, (a) V_o=250 V and P_o=1 kW, and (b) V_o=380 V and P_o=1.5 kW.

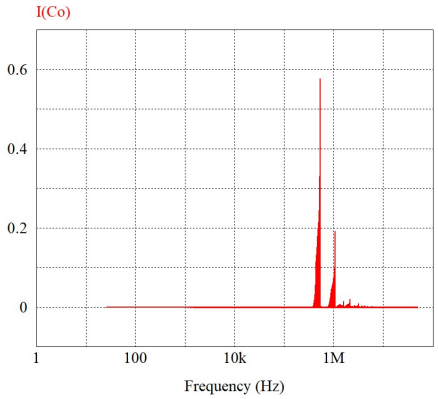

Fig. 8. Simulated FFT analysis result of the output capacitor current.

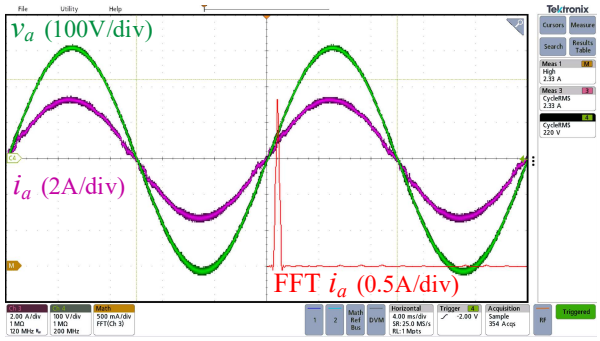

Fig. 9. Experimentally measured FFT of the input current illustrating unity power factor.

switching devices. Due to its single-stage operation with negligible switching loss, the proposed rectifier outperforms most of the conventional rectifiers. The basic operation is explained, and the potential of the proposed converter is revealed. The main operation of the proposed rectifier is verified by computer simulations and experimental results.

REFERENCES

[1] Matsumoto, A. Fukui, T. Takeda and M. Yamasaki, "Development of 400-Vdc output rectifier for 400-Vdc power distribution system in telecom sites and data centers," in *IEEE Proc. INTELEC*, Orlando, FL, 2010, pp. 1-6.

[2] T. Soeiro, T. Friedli and J. W. Kolar, "Three-phase high power factor mains interface concepts for Electric Vehicle battery charging systems," in *IEEE Proc. APEC*, Orlando, FL, 2012, pp. 2603-2610.

[3] J. W. Kolar and T. Friedli, "The essence of three-phase PFC rectifier systems," in *IEEE Proc. INTELEC*, Amsterdam, 2011, pp. 1-27.

[4] T. B. Soeiro, T. Friedli and J. W. Kolar, "Swiss rectifier — A novel three-phase buck-type PFC topology for Electric Vehicle battery charging," in *IEEE Proc. APEC*, Orlando, FL, 2012, pp. 2617-2624.

[5] J. Deng, S. Li, S. Hu, C. C. Mi and R. Ma, "Design Methodology of LLC Resonant Converters for Electric Vehicle Battery Chargers," *IEEE Trans. Veh. Technol.*, vol. 63, no. 4, pp. 1581-1592, May 2014.

[6] T. Mishima, K. Akamatsu and M. Nakaoka, "A High Frequency-Link Secondary-Side Phase-Shifted Full-Range Soft-Switching PWM DC–DC Converter With ZCS Active Rectifier for EV Battery Chargers," *IEEE Trans. Power Electron.*, vol. 28, no. 12, pp. 5758-5773, Dec. 2013.

[7] B. R. de Almeida, D. de Souza Oliveira and P. P. Praça, "A bidirectional single-stage three-phase rectifier with high-frequency isolation and power factor correction," in *IEEE Proc. APEC*, Long Beach, CA, 2016, pp. 60-65.

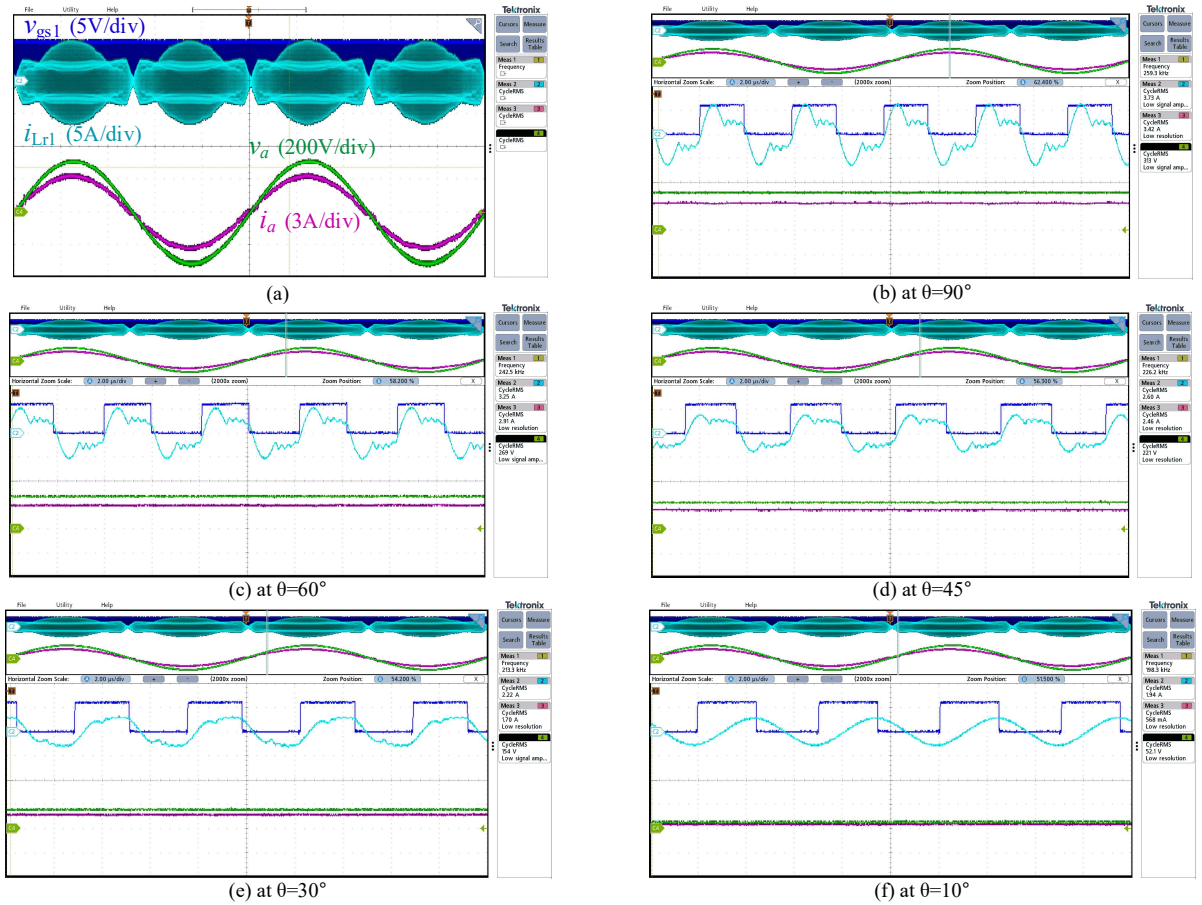

Fig. 10. Experimental results for V_o=380 V condition, (a) steady-state waveform, (b)-(f) zoomed-in views at different line phase angles (θ).

[8] D. Das, N. Weise, K. Basu, R. Baranwal and N. Mohan, "A Bidirectional Soft-Switched DAB-Based Single-Stage Three-Phase AC–DC Converter for V2G Application," *IEEE Trans. Transport. Electrific.*, vol. 5, no. 1, pp. 186-199, March 2019.

[9] K. Ali, S. K. Dube, P. Das, J. C. Peng and D. J. Rogers, "Improvement of ZVS Range and Current Quality of the Nine-Switch Single-Stage AC–DC Converter," *IEEE Trans. Power Electron.*, vol. 35, no. 5, pp. 4658-4668, May 2020.

[10] G. Tibola and I. Barbi, "Isolated Three-Phase High Power Factor Rectifier Based on the SEPIC Converter Operating in Discontinuous Conduction Mode," *IEEE Trans. Power Electron.*, vol. 28, no. 11, pp. 4962-4969, Nov. 2013.

[11] X. Zhang, L. Zhou, D. Qiu, W. Xiao, B. Zhang and F. Xie, "Phase-modular three-phase isolated bridgeless PFC converter," in *IEEE Proc. IECON,* Yokohama, 2015, pp. 001723-001728.

[12] S. Gangavarapu, A. K. Rathore and D. M. Fulwani, "Three-Phase Single-Stage-Isolated Cuk-Based PFC Converter," *IEEE Trans. Power Electron.*, vol. 34, no. 2, pp. 1798-1808, Feb. 2019.

[13] G. Bhuvaneswari, S. Narula and B. Singh, "Three-phase push-pull modular converter based welding power supply with improved power quality," in *IEEE Proc. 5th India International Conference on Power Electronics (IICPE)*, Delhi, 2012, pp. 1-5.

[14] J. Lu, K. Bai, A. R. Taylor, G. Liu, A. Brown, P. M. Johnson and M. McAmmond, "A Modular-Designed Three-Phase High-Efficiency High-Power-Density EV Battery Charger Using Dual/Triple-Phase-Shift Control," *IEEE Trans. Power Electron.*, vol. 33, no. 9, pp. 8091-8100, Sept. 2018.

[15] Yanjun Zhang, Dehong Xu, Min Chen, Yu Han and Zhoong Du, "LLC resonant converter for 48 V to 0.9 V VRM," in *IEEE Proc. 35th Annual Power Electronics Specialists Conference (PESC)*, Aachen, 2004, pp. 1848-1854 Vol.3.

[16] H. Choi, "Analysis and Design of LLC Resonant Converter with Integrated Transformer," in *IEEE Proc. APEC*, Anaheim, CA, 2007, pp. 1630-1635.

[17] C. Chang, E. Chang and H. Cheng, "A High-Efficiency Solar Array Simulator Implemented by an LLC Resonant DC–DC Converter," *IEEE Trans. Power Electron.*, vol. 28, no. 6, pp. 3039-3046, June 2013.

[18] B. Li, Q. Li and F. C. Lee, "A WBG based three phase 12.5 kW 500 kHz CLLC resonant converter with integrated PCB winding transformer," in *IEEE Proc. APEC*, San Antonio, TX, 2018, pp. 469-475.

[19] X. Zhou, B. Sheng, W. Liu, Y. Chen, A. Yurek, Y. F. Liu, P. C. Sen and K. L. V. Iyer, "A High Efficiency High Power-Density LLC DC-DC Converter for Electric Vehicles (EVs) On-Board Low Voltage DC-DC Converter (LDC) Application," in *IEEE Proc. APEC*, New Orleans, LA, 2020, pp. 1339-1346.

[20] M. Forouzesh and Y. -F. Liu, "Interleaved LCLC Resonant Converter With Precise Current Balancing Over a Wide Input Voltage Range," *IEEE Trans. Power Electron.*, vol. 36, no. 9, pp. 10330-10342, Sept. 2021.

[21] Y. Qiu, W. Liu, P. Fang, Y. Liu and P. C. Sen, "A mathematical guideline for designing an AC-DC LLC converter with PFC," in *IEEE Proc. APEC*, San Antonio, TX, 2018, pp. 2001-2008.

[22] M. Wattenberg, U. Schwalbe and M. Pfost, "Single-Stage LLC Charger with PFC Functionality and Wide Input Voltage Range," in *IEEE Proc. APEC*, Anaheim, CA, 2019, pp. 750-756.

[23] W. Liu, A. Yurek, B. Sheng, Y. Chen, Y. -F. Liu and P. C. Sen, "A Single Stage 1.65kW AC-DC LLC Converter with Power Factor Correction (PFC) for On-Board Charger (OBC) Application," in *IEEE Proc. ECCE*, Detroit, MI, 2020, pp. 4594-4601.